Research Article | Vol. 7, No. 2 | 1 Feb 2017 | OPTICAL MATERIALS EXPRESS 304

Optical Materials EXPRESS

Phosphorus doping effect on linear and nonlinear optical properties of Si/SiO_2 multilayers

PEI ZHANG,[1,2] XIAOWEI ZHANG,[1] SHUO XU,[1] PENG LU,[1] DAMENG TAN,[1] JUN XU,[1,*] FENGQIU WANG,[1] LIYING JIANG,[2] AND KUNJI CHEN[1]

[1]*National Laboratory of Solid State Microstructures, School of Electronic Science and Engineering and Collaborative Innovation Centre of Advanced Microstructures, Nanjing University, Nanjing 210093, China*

[2]*Henan Key Lab of Information-based Electrical Appliances, Department of Electrical and Information Engineering, Zhengzhou University of Light Industry, Zhengzhou 450002, China*

**junxu@nju.edu.cn*

Abstract: The linear and nonlinear optical properties of phosphorous-doped Si/SiO_2 multilayers as a function of doping concentration were investigated. It was found that the linear optical absorption became weak with the doping concentrations while the corresponding nonlinear optical absorption coefficient was reduced by 4 folds after phosphorus doping. Our experimental results demonstrated that the interface states were passivated by the phosphorus dopants which changed the chemical environment of the Si nanoclusters and in turn affected both the linear and nonlinear optical processes. The excitation-wavelength dependent nonlinear optical behaviors also supported our proposed model. It was suggested that the linear and nonlinear optical properties can be tunable via controlling the phosphorous doping concentrations which provided a new approach to improve the performance of nano-Si-based photonic devices.

OCIS codes: (190.4720) Optical nonlinearities of condensed matter; (160.4236) Nanomaterials; (230.4170) Multilayers.

References and links

1. A. Martínez, J. Blasco, P. Sanchis, J. V. Galán, J. García-Rupérez, E. Jordana, P. Gautier, Y. Lebour, S. Hernández, R. Guider, N. Daldosso, B. Garrido, J. M. Fedeli, L. Pavesi, J. Martí, and R. Spano, "Ultrafast all-optical switching in a silicon-nanocrystal-based silicon slot waveguide at telecom wavelengths," Nano Lett. **10**(4), 1506–1511 (2010).
2. L. Sirleto, M. A. Ferrara, T. Nikitin, S. Novikov, and L. Khriachtchev, "Giant Raman gain in silicon nanocrystals," Nat. Commun. **3**, 1220 (2012).
3. J. Matres, C. Lacava, G. C. Ballesteros, P. Minzioni, I. Cristiani, J. M. Fédéli, J. Martí, and C. J. Oton, "Low TPA and free-carrier effects in silicon nanocrystal-based horizontal slot waveguides," Opt. Express **20**(21), 23838–23845 (2012).
4. K. Imakita, M. Ito, M. Fujii, and S. Hayashi, "Nonlinear optical properties of phosphorous-doped Si nanocrystals embedded in phosphosilicate glass thin films," Opt. Express **17**(9), 7368–7376 (2009).
5. M. Ito, K. Imakita, M. Fujii, and S. Hayashi, "Nonlinear optical properties of phosphorus-doped silicon nanocrystals/nanoclusters," J. Phys. D Appl. Phys. **43**(50), 505101 (2010).
6. K. Ikeda, Y. Shen, and Y. Fainman, "Enhanced optical nonlinearity in amorphous silicon and its application to waveguide devices," Opt. Express **15**(26), 17761–17771 (2007).
7. P. Zhang, X. Zhang, P. Lu, J. Xu, X. Xu, W. Li, and K. Chen, "Interface state-related linear and nonlinear optical properties of nanocrystalline Si/SiO_2 multilayers," Appl. Surf. Sci. **292**, 262–266 (2014).
8. P. Zhang, X. Zhang, J. Xu, W. Mu, J. Xu, W. Li, and K. Chen, "Tunable nonlinear optical properties in nanocrystalline Si/SiO_2 multilayers under femtosecond excitation," Nanoscale Res. Lett. **9**(1), 28 (2014).
9. W. Mu, P. Zhang, J. Xu, S. Sun, J. Xu, W. Li, and K. Chen, "Direct-current and alternating-current driving Si quantum dots-based light emitting device," IEEE J. Sel. Top. Quantum Electron. **20**(4), 8200106 (2014).
10. X. D. Pi, R. Gresback, R. W. Liptak, S. A. Campbell, and U. Kortshagen, "Doping efficiency, dopant location, and oxidation of Si nanocrystals," Appl. Phys. Lett. **92**(12), 123102 (2008).
11. X. J. Hao, E.-C. Cho, G. Scardera, E. Bellet-Amalric, D. Bellet, Y. S. Shen, S. Huang, Y. D. Huang, G. Conibeer, and M. A. Green, "Effects of phosphorus doping on structural and optical properties of silicon nanocrystals in a SiO_2 matrix," Thin Solid Films **517**(19), 5646–5652 (2009).

#279996 http://dx.doi.org/10.1364/OME.7.000304
Journal © 2017 Received 7 Nov 2016; revised 20 Dec 2016; accepted 21 Dec 2016; published 4 Jan 2017

Optical Materials EXPRESS

12. B. L. Oliva-Chatelain, T. M. Ticich, and A. R. Barron, "Doping silicon nanocrystals and quantum dots," Nanoscale **8**(4), 1733–1745 (2016).
13. P. Lu, W. Mu, J. Xu, X. Zhang, W. Zhang, W. Li, L. Xu, and K. Chen, "Phosphorus doping in Si nanocrystals/SiO_2 msultilayers and light emission with wavelength compatible for optical telecommunication," Sci. Rep. **6**, 22888 (2016).
14. H. Sun, J. Xu, Y. Liu, W. Mu, W. Xu, W. Li, and K. Chen, "Subband Light Emission from phosphorous-doped amorphous Si/SiO_2 multilayers at room temperature," Chin. Phys. Lett. **28**(6), 067802 (2011).
15. P. Lu, D. Li, P. Zhang, D. Tan, W. Mu, J. Xu, W. Li, and K. Chen, "Time-resolved and temperature-dependent photoluminescence study on phosphorus doped Si quantum dots/SiO_2 multilayers with ultra-small dot sizes," Opt. Mater. Express **6**(10), 3233–3241 (2016).
16. M. Sheik-Bahae, A. A. Said, T.-H. Wei, D. A. Hagan, and E. W. Van Stryland, "Sensitive measurements of optical nonlinearities using a single beam," IEEE J. Quantum Electron. **26**(4), 760–769 (1990).
17. R. Spano, N. Daldosso, M. Cazzanelli, L. Ferraioli, L. Tartara, J. Yu, V. Degiorgio, E. Giordana, J. M. Fedeli, and L. Pavesi, "Bound electronic and free carrier nonlinearities in Silicon nanocrystals at 1550nm," Opt. Express **17**(5), 3941–3950 (2009).
18. C. Song, G. R. Chen, J. Xu, T. Wang, H. C. Sun, Y. Liu, W. Li, Z. Y. Ma, L. Xu, X. F. Huang, and K. J. Chen, "Evaluation of microstructures and carrier transport behaviors during the transition process from amorphous to nanocrystalline silicon thin films," J. Appl. Phys. **105**(5), 054901 (2009).
19. S. Zhou, X. D. Pi, Z. Y. Ni, Q. B. Luan, Y. Y. Jiang, C. H. Jin, T. Nozaki, and D. Yang, "Boron- and phosphorus-hyperdoped silicon nanocrystals," Part. Part. Syst. Charact. **32**(2), 213–221 (2015).
20. M. Perego, C. Bonafos, and M. Fanciulli, "Phosphorus doping of ultra-small silicon nanocrystals," Nanotechnology **21**(2), 025602 (2010).
21. H. Sugimoto, M. Fujii, K. Imakita, S. Hayashi, and K. Akamatsu, "Phosphorus and boron codoped colloidal silicon nanocrystals with inorganic atomic ligands," J. Phys. Chem. C **117**(13), 6807–6813 (2013).
22. H. Gnaser, S. Gutsch, M. Wahl, R. Schiller, M. Kopnarski, D. Hiller, and M. Zacharias, "Phosphorus doping of Si nanocrystals embedded in silicon oxynitride determined by atom probe tomography," J. Appl. Phys. **115**(3), 034304 (2014).
23. G. Vijaya Prakash, M. C Azzanelli, Z. Gaburro, L. Pavesi, F. Iacona, G. Franzò, and F. Priolo, "Nonlinear optical properties of silicon nanocrystals grown by plasma-enhanced chemical vapor deposition," J. Appl. Phys. **91**(7), 4607–4610 (2002).
24. S. Hernández, P. Pellegrino, A. Martínez, Y. Lebour, B. Garrido, R. Spano, M. Cazzanelli, N. Daldosso, L. Pavesi, E. Jordana, and J. M. Fedeli, "Linear and nonlinear optical properties of Si nanocrystals in SiO_2 deposited by PECVD," J. Appl. Phys. **103**(6), 064309 (2008).
25. Y. J. Ma, J. I. Oh, D. Q. Zheng, W. A. Su, and W. Z. Shen, "Tunable nonlinear absorption of hydrogenated nanocrystalline silicon," Opt. Lett. **36**(17), 3431–3433 (2011).
26. S. Vijayalakshumi, H. Grebel, G. Yaglioglu, R. Pino, R. Dorsinville, and C. W. White, "Nonlinear optical response of Si nanostructures in a silica matrix," J. Appl. Phys. **88**(11), 6418–6422 (2000).
27. M. Ito, K. Imakita, M. Fujii, and S. Hayashi, "Nonlinear optical properties of silicon nanoclusters/nanocrystals doped SiO_2 films: Annealing temperature dependence," J. Appl. Phys. **108**(6), 063512 (2010).
28. S. Dhara, K. Imakita, P. K. Giri, and M. Fujii, "Strain dependence of the nonlinear optical properties of strained Si nanoparticles," Opt. Lett. **39**(13), 3833–3836 (2014).
29. S. Minissale, S. Yerci, and L. Nero, "Nonlinear optical properties of low temperature annealed silicon-rich oxide and silicon-rich nitride materials for silicon photonics," Appl. Phys. Lett. **100**(2), 021109 (2012).
30. G. M. Dalpian and J. R. Chelikowsky, "Self-purification in semiconductor nanocrystals," Phys. Rev. Lett. **96**(22), 226802 (2006).
31. Y. Rui, D. Chen, J. Xu, Y. Zhang, L. Yang, J. Mei, Z. Ma, Z. Cen, W. Li, L. Xu, X. Huang, and K. Chen, "Hydrogen-induced recovery of photoluminescence from annealed *a*-Si:H/*a*-SiO_2 multilayers," J. Appl. Phys. **98**(3), 033532 (2005).
32. J. Mei, Y. Rui, Z. Ma, J. Xu, D. Zhu, L. Yang, X. Li, W. Li, X. Huang, and K. Chen, "Contribution of multiple emitting centers to luminescence from Si/SiO_2 multilayers with step by step thermal annealing," Solid State Commun. **131**(11), 701–705 (2004).

1. Introduction

Nonlinear optical properties of nanocrystalline-Si (nc-Si) materials have recently attracted great interest due to its large optical nonlinearities, which can be applied in many kinds of Si-based photonic devices such as optical switch, Raman amplifier and optical waveguide [1–3]. The all-optical switch at speeds well above 40 Gbit/s was fabricated based on the nano-Si material, but its modulation depth was relative low compared with that based on bulk silicon [1]. In order to improve the device performance, it is necessary to enhance the Kerr coefficient by controlling the materials structures such as dot size and the chemical environment of nano-dots. M. Fujii et al. reported that the nonlinear refractive indices of nc-Si were strongly enhanced through impurity-doping (phosphorus) due to the impurity-relate

Optical Materials EXPRESS

states [4,5]. However, the two photon absorption (TPA) was also increased which will influence the device performance since the longer free carries effect generated by single or two photon absorption will overwhelm the instantaneous Kerr effect, thus lowering the switching speed. Moreover, K. Ikeda et al. found that the introduction of midgap localized states in Si-based materials can significantly reduce the lifetime of free-carries while the corresponding optical loss was enhanced [6], because the induced defect states will increase the light scattering and optical loss [1]. In our previous work, the linear and nonlinear optical properties of un-doped nc-Si/SiO_2 multilayers were systematically studied [7–9]. The nonlinear optical behaviors can be explained as the interface state-related two-step absorption process and the large nonlinear optical response was observed which was strongly dependent on the interface states by changing the nc-Si dot size or post-annealing temperatures [7,8]. Doping of nc-Si is another effective way to modify the chemical environment of nc-Si surfaces. It was found that phosphorus (P)-dopants can passivate the surface defects such as dangling bonds and reconstruct the surface chemical bonds [10–13], which may produce a new approach to control the linear and nonlinear optical properties of nc-Si materials.

In the present work, we employed phosphorous-doping to modify the interfacial condition and achieved precise tuning of the linear and nonlinear optical properties of Si/SiO_2 multilayers. The microstructures of Si/SiO_2 multilayers after P-doping and high temperature annealing were characterized. The nonlinear optical properties were investigated by Z-scan technique, and the dependence of nonlinear optical absorption on the P doping concentrations as well as excitation wavelength was measured, the tunable nonlinear absorption behaviors were obtained. Our results suggested that interfacial environment can be effectively changed by the P-doping and will lead to effective suppression of the nonlinear optical absorption.

2. Experimental

The phosphorous-doped hydrogenated amorphous Si/SiO_2 (P-doped *a*-Si:H/SiO_2) multilayers structures with 9 periods were fabricated in conventional plasma-enhanced chemical-vapor (PECVD) system, details of preparation condition can be found elsewhere [13–15]. A SiH_4 flow rate was kept at 5 SCCM, while the different P doping concentration in the *a*-Si layers were controlled by varying the gas flow ratio R (R = [PH_3] / [SH_4]). Here after, we denoted the sample prepared by R = 0, 0.2, 1, 2, 3 samples as sample A, B, C, D and E, respectively. Then, the as-deposited samples were dehydrogenated at 450 °C for 1 hour, and followed by 1 hour annealing in pure N_2 atmosphere at temperatures 800 and 900 °C. The microstructures of multilayers were characterized by cross-sectional transmission electron microscopy (X-TEM) and Raman scattering spectroscopy. Optical absorbance spectra were estimated through Shimazu UV-3600 spectrophotometer and the measured wavelength regions were from 300 to 1500 nm.

The Z-scan technique [16] was applied to measure the nonlinear optical absorption coefficients of phosphorous-doped Si/SiO_2 multilayers. In this experiment, the excitation laser was a mode-locked Ti: sapphire laser (Coherent Libra-HE) with 100-fs pulse duration at 800 nm, the repetition rate was kept at 1 kHz. The low repetition rate is in favor of reducing the thermal accumulative effect [17]. A lens with 20 cm focal length was used to obtain Gaussian beam and focused on the samples, the obtained beam waists was about 20 μm. The tunable wavelengths were generated by using an optical parametric amplifier (Opera Solo) coupled to the Ti: sapphire laser (Coherent Libra-HE).

3. Results and discussion

Figure 1(a) is the X-TEM of sample D annealed at 800 °C and the periodic structures are clearly identified. It is shown that the high density of nanocluster with average size of 2 nm is formed in amorphous Si film. However, the ultra-small dots are still amorphous phase, because of no lattice fringes could be observed from its high-resolution TEM (HRTEM). Moreover, when the annealing temperature is increased to 900 °C, the small amorphous

Optical Materials EXPRESS

nanoclusters have crystallized into nc-Si as shown in the Fig. 1(b). The lattice fringes could be clearly identified according to the HRTEM (as illustrated in the inset of Fig. 1(b)).

Figure 2(a) shows the Raman spectra of samples A-E annealed at 800 °C. All samples exhibit a broad band around 480 cm^{-1}, which is related to the TO mode of amorphous Si phase. The Raman intensity for sample E is the smallest while the Raman intensity of other samples is comparable. It looks like that the density of nanocluster is the lowest in sample E. Figure 2(b) displays the samples A-E annealed at 900 °C. It is interesting to note that the crystallinity can be enhanced with increasing the P concentration. For sample A, a weak shoulder at about 517 cm^{-1} emerges, indicating the existence of crystalline phase. The calculated crystallinity in sample A is about 19%. A sharp peak centered at 517.3 cm^{-1} is clearly identified for sample D and E and the corresponding crystallinity for samples D and E reach up to 68% and 71%, respectively, which means the crystallization is promoted in samples with high P doping concentrations. However, the size of nc-Si dots is not changed with increasing the doping concentration due to the limitation of the SiO_2 layers, which is also confirmed by the X-TEM observations.

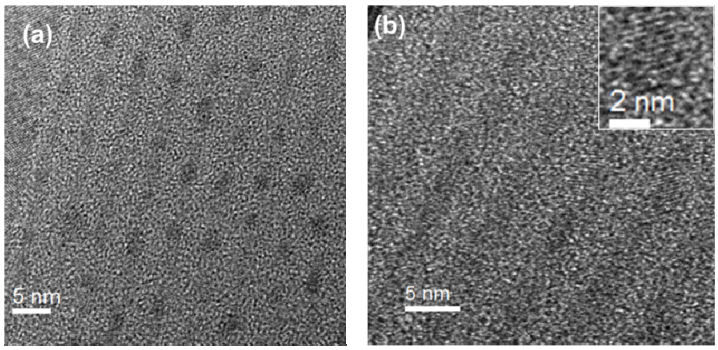

Fig. 1. X-TEM micrograph of sample D annealed at (a) 800 °C and (b) 900 °C. Inset is the HRTEM of nc-Si.

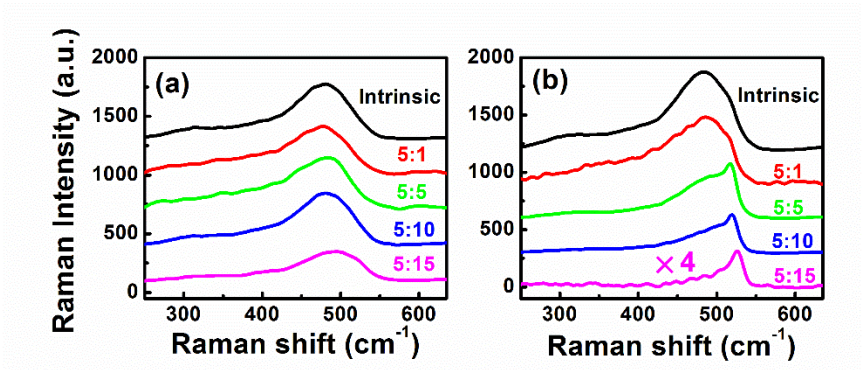

Fig. 2. Raman spectra of samples A-E annealed at (a) 800 °C and (b) 900 °C.

Figure 3(a) represents the linear optical absorption spectra of samples A-E after 900 °C annealing. It is shown that all optical absorption spectra are quite weak in the near-infrared region, while the absorbance rapidly increases when the wavelength is shorter than 500 nm. Meanwhile, the optical absorption edge shifts to the high energy with increasing the doping concentration, representing the bandgap of Si/SiO_2 multilayers enlarges after P-doping. The optical bandgaps could be estimated according to the Tauc plots and the optical bandgap is 2.0, 2.1, 2.3, 2.4 and 2.6 eV for samples A-E, respectively. It was reported previously that the grain boundaries may induce the increase of bandgap in the samples with high crystallinity

Optical Materials EXPRESS

[18]. Meanwhile, introduction of P impurities in nc-Si can promote the oxidation [19], i.e. during the annealing process. Therefore, the increase of the Si oxide content could be also responsible for the enlargement of the optical bandgap [11], which was observed in our nc-Si/SiO_2 multilayers.

The optical absorbance at 800 nm as a function of P concentration is plotted in Fig. 3(b), both sets of optical absorbance show a gradual decrease as the doping concentration increased. It is found that the optical absorption edge for samples annealed at 900 °C is blue-shifted for samples compared with those after 800 °C annealing (not shown here). As a consequence, the absorbance of 800 °C annealed samples is higher than that of 900 °C annealed ones. The absorbance of Si-based materials in near-infrared region usually arises from the localized states located at the midgap [6–8]. In our previous work, it was found that part of P atoms were located at the interface of Si/SiO_2 to passivate the dangling bond (DB) on the nc-Si surface and terminate the corresponding defect states [13]. Meanwhile, the P-Si/P-O bond could be formed at the interface which can modify the chemical environment of Si dots [11,13,19–22]. Therefore, the absorption related to the midgap states generated by DB bonds or Si-O bonds declines with increasing the P doping concentration. Note that no obvious infrared absorption originated from the intra-valence-band transition was measured.

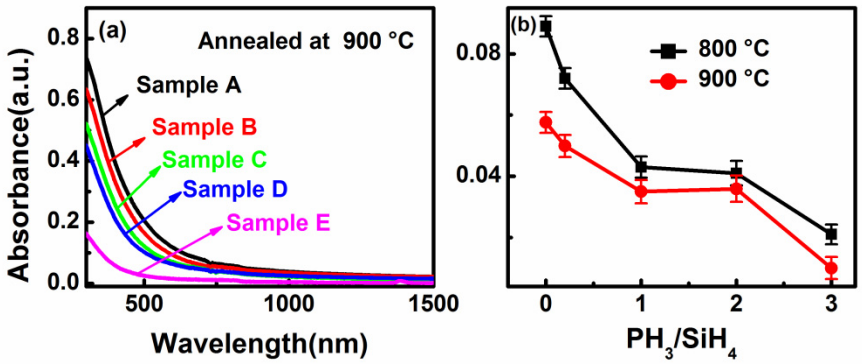

Fig. 3. (a) Optical absorbance spectra of samples A-E annealed at 900 °C. (b) The optical absorbance of all samples at 800 nm as a function of P concentration. The lines are the guided to the eye.

In order to further investigate the effect of phosphorus-doping effect on the nonlinear optical response of Si/SiO_2 multilayers, the Z-scan measurements with open aperture were carried out. Figures 4(a)-4(f) shows the normalized Z-scan transmittance traces of samples A, D and E in the open aperture configuration under laser intensity $I_0 = 4.78 \times 10^{10}$ W/cm^2 at 800 nm. It is evident that all the Z-scan traces show a dip at the focal point. The nonlinear absorption coefficient β can be extracted by fitting the measured transmittance data according to the following equation [17],

$$T = 1 - \frac{1}{2\sqrt{2}} \frac{\beta I_0 L_{eff}}{x^2 + 1}. \quad (1)$$

where $x = z / z_0$, $z_0 = k\omega_0^2 / 2$ and z are the Rayleigh diffraction length and the sample position from the focal point, respectively. I_0 indicates the excitation intensity at the focal point, L_0 is the effective thickness of the sample, α_0 and L are the linear absorption coefficient and the real thickness of sample, respectively.

Optical Materials EXPRESS

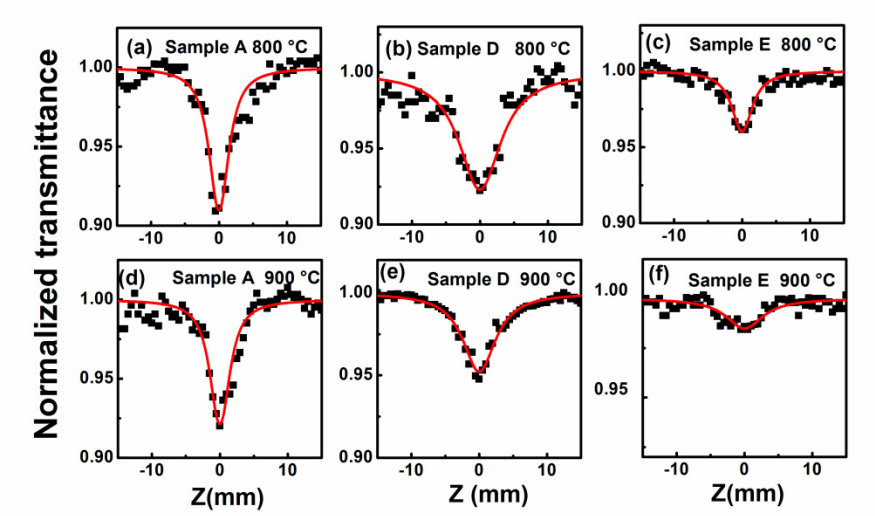

Fig. 4. Open aperture Z-scan traces of samples A, D and E annealed at (a)-(c) 800 °C and (d)-(f) 900 °C. The excitation wavelength and intensity are 800 nm and $I_0 = 4.78 \times 10^{10}$ W/cm^2, respectively. The solid lines are the fitting curves of the experimental data.

It is found that the transmittance at focus enhanced with increasing the annealing temperature, indicating that reduction of the nonlinear absorption (NLA). The dependence of NLA β on P concentration is displayed in Fig. 5(a). For samples annealed at 900 °C, the NLA β monotonously decreases from 4.20×10^{-7} to 1.04×10^{-7} cm/W with increasing P doping concentrations. The variation characteristic of nonlinear absorption with doping concentration and annealing temperature is similar with the linear optical absorption as depicted in Fig. 3(b). Moreover, the wavelength dependence of NLA β for samples A and D was also measured as plotted in Fig. 5(b), the inset shows the linear optical absorption in the range of 800-1400 nm. The linear and nonlinear absorption as a function of wavelength exhibit the similar trend, and they decrease with increasing the excitation wavelength. This behavior is further confirmed the fact that the linear absorption have a significant effect on the nonlinear absorption process.

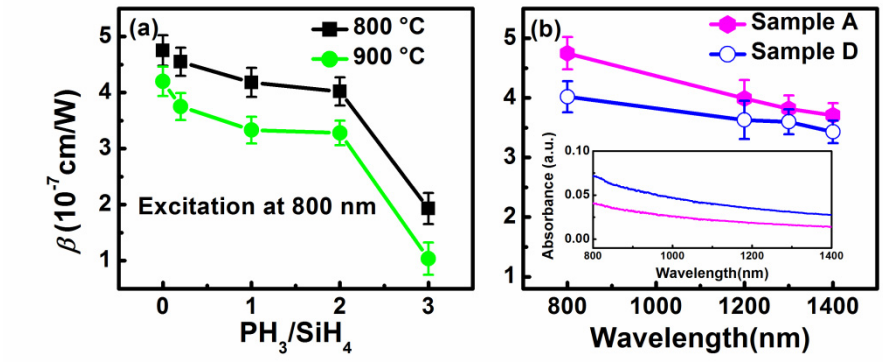

Fig. 5. The nonlinear absorption coefficient β as function of (a) P doping concentration and (b) the excitation wavelength. The inset is the optical absorbance spectra of samples A and D annealed at 800 °C ranged from 800 nm to 1400 nm.

So far, the originations of nonlinear optical effect on Si-based materials are still in controversial [7,17,23–29]. The quantum confined effect is ascribed to the large nonlinear

Optical Materials EXPRESS

optical response due to the size-dependent characteristics [17,24,25]. However, some groups reported that the localized defect states play a great role in the nonlinear optical process [7,26–29]. In our previous reports, the nonlinear optical properties of intrinsic Si/SiO_2 multilayers were investigated by using the Ti: sapphire laser with 50 fs pulse duration at 800 nm [7,8]. The nc-Si dots with average size of 4 nm were prepared, the nonlinear absorption turns the reverse saturation absorption (RSA) into saturation absorption (SA) with increasing the annealing temperature to make the sample change from amorphous phase to nanocrystalline state [8]. The RSA was ascribed to TPA process, while we attributed the SA to the phonon-assisted one-photon transition process between the valence band and interface states. However, the NLA process changed when the size of nc-Si dot is 2.5 nm, the two-step absorption through the interface states in the midgap dominated the NLA process [7]. Because of the larger surface-to-volume ratio, much more interface states were introduced in the gap, which is confirmed by the PL measurements, the sample with size of 2.5 nm displays stronger PL intensity (about 10 times) than that with 4 nm. In the present work, the size of nc-Si dot is about 2 nm and excitation intensity ($I_0 = 4.78 \times 10^{10}$ W/cm^2) is lower than that in the ($I_0 = 3.54 \times 10^{11}$ W/cm^2). In this case, we considered that the NLA process of all samples was still dominated by the two-step absorption via interface states, and the obtained NLA coefficients are also positive. The density of midgap states as well as optical bandgap plays a major role in the nonlinear optical absorption of Si-based materials [7,8,26–29]. Therefore, we discuss the nonlinear optical behavior of P-doped Si/SiO_2 multilayers based on the two factors.

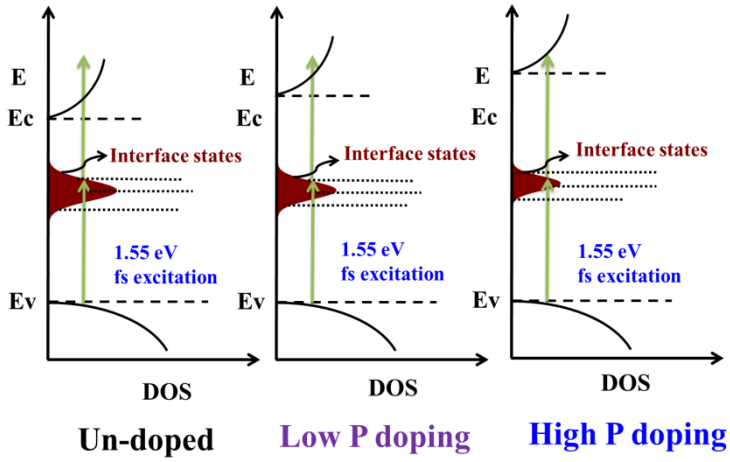

Fig. 6. The schematic diagrams of optical nonlinear transition process. The left graph is the two-step absorption process via the interface states for the un-doped sample, the middle and right diagrams demonstrate the reduction of the density of interfaces states and the widening of the bandgap with low and high P doping.

One is the change of interface states after P-doping. It is found that the dependence of linear and nonlinear optical absorption on the doping concentration is similar, which can be attributed to the reduced interface states after P doping. K. Imakita et al. studied the linear and nonlinear absorption coefficients of nc-Si as function of the P concentration and they found that nonlinear optical absorption coefficient was increased with increasing the doping concentration, which is contrary to our observations [4,5]. The difference may arise from the different role of the P atoms in nc-Si materials prepared by two different preparation methods. Since the average dot size is about 4 nm in references [4,5], and P atoms can occupy the inner sites in Si nano-dots and form the impurity-related energy levels below the conduction band after P doping and hence the linear and nonlinear optical absorption can be

Optical Materials EXPRESS

enhanced due to the increased midgap states. In our case, the dot size is quite small (~2nm), the impurities are difficult to enter into the Si nano-dots due to the self-purification effect and the most of P atoms tend to stay at the interfacial region [13,30], leading to the passivation of the DB and re-construct the surface chemical bonds. Therefore, the density of midgap states decreases with increasing the P doping concentrations as schematically illustrated in Fig. 6, which results in the reduction of both the linear and nonlinear optical absorption at near-infrared region since the reduction of midgap states makes the NLA process via two step absorption become weaken. K. Ikeda et al. attributed the large reverse saturation absorption coefficient to the two step absorption through the midgap states generated by the DB defect, and the density of the midgap states could be tuned by introducing the hydrogen since hydrogen is also able to passivate the DB [6,31], which is similar with our results.

The reduction of interface states can be confirmed by the change of photoluminescence behaviors. It was found that the PL band around 800-900 nm (Band I) can be detected not only from un-doped sample but also P-doped ones. This emission band was usually attributed to the radiative recombination of photo-generated electron-hole pairs via interfaces states located at the nc-Si/SiO_2 interfacial region [9,31,32]. It was found that the peak position and spectral shape is almost the same, but their intensities are gradually decreased with P doping [13], which suggested the reduction of interface states due to the P passivation effect. It was further supported by the XPS spectra and ESR measurements that the P atoms tend to exist at interfacial region and may passivate the surface states of nc-Si effectively. It was also found that P doping may generate the deep levels in nc-Si and another emission band (Band II) centered at 1300 nm can be detected. The emission intensities are increased with P doping to the certain concentrations. However, it should be noted that, although the deep levels are introduced in the gap of Si quantum dots through P doping, no apparent absorption related to the deep states can be found at around 1300 nm according to the linear absorption spectra displayed in Fig. 3(a).

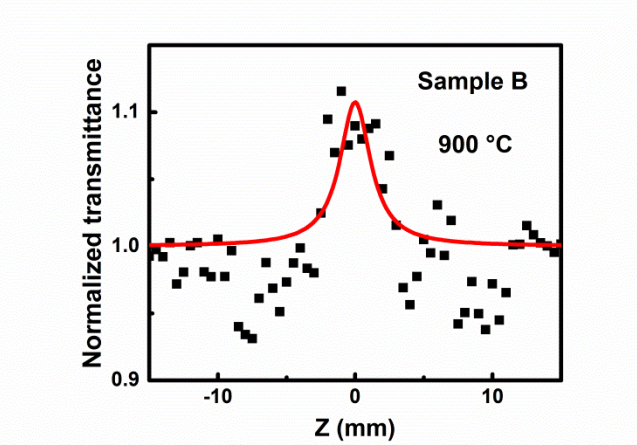

Fig. 7. Open aperture Z-scan curve of sample B annealed at 900 °C. The excitation wavelength and intensity are 800 nm and $I_0 = 2.79 \times 10^{11}$ W/cm^2, respectively. The solid line is the fitting curve of the experimental data.

To further understand the role of interface states in NLA process, the intensity-dependent NLA properties are investigated. The typical one is sample B as shown in Fig. 7. When the excitation intensity is increased up to the $I_0 = 2.79 \times 10^{11}$ W/cm^2, the NLA changes from reverse saturation absorption ($I_0 = 4.78 \times 10^{10}$ W/cm^2) to saturation absorption, which is the similar with that in the un-doped nc-Si/SiO_2 multilayers we reported previously [8]. Under higher pump intensity, much more electrons are excited and all the interface states are fully occupied. Therefore, the saturation absorption occurs due to the state-filling effect, which

Optical Materials EXPRESS

indicates that the interface state-related two-step absorption mechanism dominates the NLA process since it cannot be observed in the two-photon absorption process.

The other one is the change of the optical bandgap after doping. It was reported that the NLA is sensitive to the bandgap, the NLA could be changed by tuning the optical bandgap of nc-Si materials [8,25]. In our case, it is found that the optical absorption edge continues to move toward the high energy with increasing P doping concentration as shown in Fig. 3(a), which means that the optical bandgap of Si/SiO_2 multilayers enlarged after P doping. As illustrated in Fig. 6, the number of absorbed photon via two step absorption process will be reduced under the same pump photon energy due to the decrease of the density states in the conduction band. Therefore, the NLA β decreased with increasing the doping concentration. To further validate the effect of the bandgap on the nonlinear optical absorption process, NLA β as function of wavelength was measured as plotted in Fig. 5(b). It is shown that the NLA β decreases as the pump wavelength increases (reduction of the excitation energy), which equally to the enlargement of the bandgap.

It should be pointed out that the annealing temperature also plays an important role in the linear and nonlinear absorption process of Si/SiO_2 multilayers. As mentioned above, high temperature annealing (900 °C) results in the improved crystallinity according to the Raman spectra as shown in Fig. 2 and the optical absorption edge for samples annealed at 900 °C is blue-shifted for samples compared with those after 800 °C annealing. Meanwhile, a large amount of P atoms are intensively moving in or at the surface of the Si NCs during the high annealing process [15]. Therefore, the optical bandgap is enlarged and interface states is reduced and both the linear and nonlinear absorption coefficients for samples annealed at 900 °C were lower than those annealed at 800 °C, as displayed in Fig. 2(b) and Fig. 5(a) consequently, which is in accordance with the model of the NLA process as shown in Fig. 6.

4. Conclusion

The P-doped Si/SiO_2 multilayers with dot size of 2 nm were fabricated in PECVD system. The crystallinity of Si/SiO_2 multilayers could be enhanced with increasing annealing temperature and doping concentration. The optical nonlinearities of P-doped Si/SiO_2 multilayers were investigated by the open aperture Z-scan technique utilizing femtosecond pulses. The NLA coefficients β could decrease as much as 4 times through P-doping. We also demonstrated that both linear and nonlinear optical absorption are doping concentration and wavelength dependent. The tunable linear and nonlinear optical absorption properties can be understood in term of the modified interface states and optical bandgap through controlling the doping concentration, which indicates that doping is a new approach to control the linear and nonlinear optical process in Si nano-dots materials and to improve the related device performance.

Funding

National Natural Science Foundation of China (No. 11274155); “973 Project (2013CB632101); “333 Project” of Jiangsu Provence (BRA2015284); and the Doctoral Foundation of Zhengzhou University of Light Industry (2014BSJJ041).